Letters

International Journal of Bifurcation and Chaos, Vol. 8, No. 11 (1998) 2203–2213

AN ALGORITHM FOR ESTIMATING FIXED POINTS OF DYNAMICAL SYSTEMS FROM TIME SERIES

LUIS A. AGUIRRE*,†,‡ and ÁLVARO V. P. SOUZA†
†*Centro de Pesquisa e Desenvolvimento em Engenharia Elétrica,*
‡*Departamento de Engenharia Eletrônica,*
Universidade Federal de Minas Gerais, Av. Antônio Carlos 6627,
31270-901 Belo Horizonte, M.G., Brazil

Received February 21, 1998; Revised April 8, 1998

This paper presents an algorithm for estimating fixed points of dynamical systems from time series. In some cases the new procedure can accurately estimate fixed points of which there is very little information in the data. Another advantage is that, although no prior knowledge is assumed, the new algorithm permits the user to employ *a priori* information about the system such as symmetry and the existence of a trivial fixed point. The new algorithm is tested on the Lorenz and Rössler systems and on real data taken from Chua's circuit.

1. Introduction

Given a nonlinear dynamical model of a system, one of the first steps in the analysis is the location of fixed points [Chen, 1998]. In the case of continuous time systems, that is $\dot{x} = f(x)$, the fixed points are defined as the solutions of $f(x) = 0$. For discrete-time systems which are of the form $x(k) = g(x(k-1))$, the fixed points are defined as the solutions of such a map with $x(k) = x(k-1)$. To locate the fixed points of a system is usually important in order to understand the global behavior of such a system. This has prompted the development of numerical algorithms to compute fixed points of Poincaré maps or of ordinary differential equations [Fujisaka & Sato, 1997].

A slightly more difficult problem is that of estimating the fixed points of a dynamical system just from some measured data. This, of course, has a number of extra difficulties such as the estimation of fixed points which are located in regions of the state space which are hardly visited by the data.

An algorithm for estimating the fixed points of a system from measured data has been proposed by Glover and Mees [1992]. Such an algorithm is based on parameter estimation for linear models and works well if the data remain close to all the fixed points in state space for a sufficiently long time. For instance, in the case of Chua's double scroll attractor, such algorithm estimates well the nontrivial fixed points, whereas the trivial fixed point is hardly detected [Glover & Mees, 1992].

The main objective of this paper is to propose a new algorithm for estimating fixed points of a dynamical system from a set of measured data. One of the differences with respect to the algorithm suggested in [Glover & Mees, 1992] is that in this work the mathematical structure is nonlinear instead of linear. This confers to the new algorithm two interesting features, viz. (i) the user can employ *a priori* knowledge which might be available from the systems (e.g. fixed point symmetry and the existence of a trivial fixed point), and (ii) the algorithm can estimate with greater facility fixed points of which there is little information in the data.

The paper is organized as follows. In the next section the main motivation for the new algorithm

*E-mail: aguirre@cpdee.ufmg.br

is presented. Section 3 deals with the estimation of fixed points. In this section, the algorithm proposed in [Glover & Mees, 1992] is reviewed and the new algorithm is described in detail. Section 4 discusses some numerical examples. The main points of the paper are summarized in Sec. 5.

2. Motivation and Background

The new algorithm presented in this paper is motivated by the fact that given a global nonlinear model estimated from data, it is usually possible to get rather accurate estimates of the fixed points of the underlying dynamics. In particular, for nonlinear discrete polynomial models the mathematical relations between model and fixed points are *very* simple [Aguirre & Mendes, 1996].

The preceeding paragraph naturally points to a two-step procedure for fixed point estimation, viz. (i) estimate a global model from the data, and (ii) determine the fixed points of the model. This procedure is, of course, totally viable but it should be realized that the first step is usually a nontrivial task and very elaborate algorithms are usually employed.

However, if all we want is to estimate fixed points from time series, it is natural to inquire if the estimation of a global nonlinear model is a compulsory step. Section 3.2 will make it clear that the answer to the previous question is negative.

The basic motivation for the present algorithm is to estimate fixed points from data *and* a "clustered mathematical nonlinear structure" which is actually an algebraic equation. Such a structure will usually have very few terms. Therefore, the algorithm being suggested is also a two-step procedure with the *vital* difference that instead of having to estimate a global nonlinear model, all that is required is to estimate few parameters (usually four or less) of an algebraic nonlinear equation.

This algorithm has one great advantage compared to the procedure based on global nonlinear model building, namely simplicity. To see this, it is important to realize that in estimating a global nonlinear model, the number of possible structures is practically "endless". Consider a simple situation in which there are, say, fifty possible regressors to be included in the model. For the sake of argumentation, assume that the "optimum" number of terms for such a model is fifteen. In how many different ways can the fifty candidate regressors be organized in groups of fifteen? But in real practice, the "optimum" number of terms is never known and many possibilities are usually tested. Also, it is *very* usual to have hundreds of candidate regressors and not just fifty. Thus it should become clear to the reader that the problem of determining the structure of a global nonlinear model is a monumental task for which rather elaborate algorithms exist ([Aguirre & Billings, 1995] and references therein).

In the proposed algorithm the need for structure selection is *completely eliminated*. As will be discussed in detail, the clustered mathematical structure has a reduced number of terms and, in some cases, one or two of them can be suppressed. Also, when it comes to parameter estimation, all that is required is the inversion of a matrix of reduced dimension (usually four or less!). A final advantage of the new algorithm, compared to the estimation of global models, is that the dynamics of the latter are quite sensitive to bias in the parameters. To avoid bias moving average terms are usually included resulting in (i) an even greater number of possible model structures, and (ii) the need for iterative estimation algorithms. As illustrated by the examples, the new algorithm is surprisingly robust with respect to noise therefore dispensing with the need for moving average terms and iterative estimation algorithms, although such a procedure cannot be ruled out should severe bias occur.

2.1. *Term clusters and fixed points*

The deterministic part of a polynomial NARMAX model can be expanded as the summation of terms with degrees of nonlinearity in the range $1 \leq m \leq \ell$. Each mth-order term can contain a pth-order factor in $y(k-n_i)$ and a $(m-p)$th-order factor in $u(k-n_i)$ and is multiplied by a coefficient $c_{p,m-p}(n_1, \ldots, n_m)$ as follows

$$y(k) = \sum_{m=0}^{\ell} \sum_{p=0}^{m} \sum_{n_1,n_m}^{n_y,n_u} c_{p,m-p}(n_1, \ldots, n_m) \times \prod_{i=1}^{p} y(k-n_i) \prod_{i=p+1}^{m} u(k-n_i)\,, \quad (1)$$

where

$$\sum_{n_1,n_m}^{n_y,n_u} \equiv \sum_{n_1=1}^{n_y} \cdots \sum_{n_m=1}^{n_u}\,, \quad (2)$$

and the upper limit is n_y if the summation refers to factors in $y(k-n_i)$ or n_u for factors in $u(k-n_i)$.

For the sake of presentation, suppose that T_s is short enough such that $y(k-1) \approx y(k-2) \approx \cdots \approx y(k-n_y)$ and $u(k-1) \approx u(k-2) \approx \cdots \approx u(k-n_u)$ then Eq. (1) can be rewritten as

$$y(k) \approx \sum_{n_1,n_m}^{n_y,n_u} c_{p,m-p}(n_1,\ldots,n_m) \times \sum_{m=0}^{\ell} \sum_{p=0}^{m} y(k-1)^p u(k-1)^{m-p}\,. \quad (3)$$

It is pointed out that the assumption made above is for the purpose of presentation only. In practice, cluster analysis can be performed without assuming oversampling. Also, considering an asymptotically stable model in steady-state, term clustering occurs *exactly* irrespective of T_s.

Definition 2.1. [Aguirre & Billings, 1995]. $\sum_{n_1,n_m}^{n_y,n_u} c_{p,m-p}(n_1,\ldots,n_m)$ in Eq. (3) are the coefficients of the *term clusters* $\Omega_{y^p u^{m-p}}$, which contain terms of the form $y(k-i)^p u(k-j)^{m-p}$ for $m = 0,\ldots,\ell$ and $p = 0,\ldots,m$. Such coefficients are called *cluster coefficients* and are represented as $\Sigma_{y^p u^{m-p}}$.

For details about the definition of term clusters and cluster coefficients the reader is referred to [Aguirre & Billings, 1995]. For the time being it suffices to realize that a term cluster is a set of terms of the same type and the respective cluster coefficient is obtained by the summation of the coefficients of all the terms of the respective cluster which are contained in the model. In practice it will be helpful to notice that terms of the same cluster explain the same type of nonlinearity.

All the possible clusters of an autonomous polynomial with degree of nonlinearity ℓ are Ω_0 = constant, Ω_y, $\Omega_{y^2},\ldots,\Omega_{y^\ell}$. Thus, the fixed points of a map with degree of nonlinearity ℓ, see Eqs. (1) and (2), are given by the roots of the following clustered polynomial

$$y(k) = c_{0,0} + y(k)\sum_{n_1=1}^{n_y} c_{1,0}(n_1) + y(k)^2 \sum_{n_1,n_2}^{n_y,n_y} c_{2,0}(n_1,n_2) + y(k)^\ell \sum_{n_1,n_\ell}^{n_y,n_y} c_{\ell,0}(n_1,\ldots,n_\ell)\,. \quad (4)$$

Finally, using the definition of cluster coefficients and dropping the argument k, the last equation can be rewritten as follows

$$y = \Sigma_{y^\ell}\, y^\ell + \cdots + \Sigma_{y^2}\, y^2 + \Sigma_y\, y + \Sigma_0\,, \quad (5)$$

where $\Sigma_0 = c_{0,0}$. From the last equation it becomes clear that an autonomous polynomial with degree of nonlinearity ℓ will have ℓ fixed points if $\Sigma_{y^\ell} \neq 0$.

In many practical situations $\Sigma_0 = c_{0,0} = 0$ and in this case the previous equation can be rewritten as

$$[\Sigma_{y^\ell}\, y^{\ell-1} + \cdots + \Sigma_{y^2}\, y + (\Sigma_y - 1)]\, y = 0\,. \quad (6)$$

From Equation (6) it becomes evident that the respective dynamical model has one trivial and $\ell-1$ nontrivial fixed points.

3. Fixed Point Estimation

This section is concerned with the estimation of fixed points from a time series. First, an algorithm based on a linear model structure will be revisited [Glover & Mees, 1992]. In the sequel, a new algorithm will be developed and discussed in detail. As will be shown, the new algorithm overcomes some shortcomings of other techniques.

3.1. *A linear model-based estimation algorithm*

A simple fixed point estimation algorithm has been presented in [Glover & Mees, 1992]. Roughly, such an algorithm is based on the following assumptions: (i) "Trajectories that pass near fixed point mimic this behavior by remaining relatively constant for a short period of time." [Glover & Mees, 1992], (ii) the system is noise-free, and (iii) in the vicinity of the fixed point the system can be described by a linear autoregressive model. Let us represent such a model as

$$y(k) = c_0 + \sum_{j=1}^{n_y} c_j\, y(k-j)\,, \quad (7)$$

with $c_0 = 1$, n_y equals the dimension of the system *locally* in the vicinity of the fixed point. Model (7) has n_y+1 unknown parameters $\Theta^{\mathrm{T}} = [c_0\ c_1\ \ldots\ c_{n_y}]$ thus if $n_y + 1$ constraints are taken, the parameter vector can be determined as

$$\Theta = \Psi^{-1}\mathbf{y}\,, \quad (8)$$

where $\Psi \in \mathbb{R}^{n_y+1 \times n_y+1}$ is assumed to be nonsingular and $\mathbf{y}^{\mathrm{T}} = [y(k)\ y(k+1)\ \ldots\ y(k+n_y-1)]$. Clearly, the fixed point, $\overline{y}$, of Eq. (7) can be obtained taking $\overline{y} = y(k) = y(k+1) = \cdots = y(k+n_y-1)$, and as $c_0 = 1$, then

$$\frac{1}{\overline{y}} = 1 - \sum_{j=1}^{n_y} c_j \,. \tag{9}$$

Hence given a window of data, Eqs. (8) and (9) can be used to estimate the fixed point. As pointed out in [Glover & Mees, 1992], in order to estimate the fixed point, the window of data should be somewhat close to such a fixed point.

The procedure outlined above can then be repeated for a window moving along a time series of a system with several fixed points. As the moving window approaches a fixed point of the system, Eq. (9) would then estimate the location of such a fixed point. However, if the data do not spend enough time close to a certain fixed point, such a singularity will be virtually invisible to the algorithm. This is one problem which can be sometimes overcome by the procedure described in the following section.

3.2. *The new fixed point estimation algorithm*

The new algorithm consists basically of two steps which are performed several times over a window that is moved along the data. In the first stage only a limited number of parameters are estimated from the data. In the second stage, cluster information and fixed point locations are calculated from such parameters. The complete procedure can be summarized as follows.

Step 1. Given a time series $\{\overline{y}(k)\}_1^N$ adequately sampled, nomalize the data by dividing each observation by the largest observation in the series, that is $\{y(k)\}_1^N = \{\overline{y}(k)\}_1^N / \max\{\overline{y}(k)\}$.

Step 2. Choose a window length L which should be wide enough to roughly cover the region in embedding space onto which the data fall. L should be smaller than N.

Step 3. Set $i = 0$.

Step 4. For the data window $\{y(k)\}_{(1+i)}^{L+i}$ build the matrix $\Psi \in \mathbb{R}^{L \times n_\theta}$ and the vector $\mathbf{y}$, according to (10) and (11), respectively.

Step 5. Estimate the parameters by least squares, that is, calculate $\hat{\Theta} = [\Psi^{\mathrm{T}}\Psi]^{-1}\Psi^{\mathrm{T}}\mathbf{y}$.

Step 6. Determine the cluster coefficients Σ_0, Σ_y, Σ_{y^2} and Σ_{y^3} according to (4).

Step 7. Determine the model fixed points, this is equivalent to calculating the roots of the polynomial (5). Plot the values of the estimated fixed points.

Step 8. Update $i = i + \Delta$ and return to Step 4 until the end of the time series is reached. Δ is the number of samples by which the data window will be shifted.

Step 9. Based on the cluster coefficient graphs decide if there are any *spurious* clusters (see examples for details). If no cluster seems spurious, then the final values of the estimated fixed points can be obtained from the plots, e.g. taking the average value. Multiply the estimated values by $\max\{\overline{y}(k)\}$ to account for the normalization performed in Step 1. If there seems to be any spurious clusters, delete such clusters from the regressor matrix Ψ and return to Step 4.

3.2.1. *Remarks on the new algorithm*

Remark 1. The sampling time of the time series is not a critical issue here unlike many other problems in state space reconstructions. However, the choice should be made following available results [Aguirre, 1995; Kugiumtzis, 1996].

Remark 2. The normalization performed in Step 1 is helpful to recognize spurious clusters in the last step. Normalization would otherwise be unnecessary. Spurious clusters are recognized by small or oscillating parameters, estimated and plotted in Step 7 [Aguirre & Billings, 1995].

Remark 3. The requirement $L < N$ in Step 2 is to allow sliding the window along the entire time series. In practice $L > 200$ works well in general.

Remark 4. It should be noted that the matrix (10) only includes a relatively small number of combinations of monomials, that is n_θ is small (typically

less than fifteen).[1] In fact, that is one of the great advantages of this algorithm, namely that the estimated fixed points are definitely *not* sensitive on which particular monomials are used to compose the $\ell+1$ columns of Ψ. Extensive simulations with very different alternatives have been carried out to support the last assertion. A more theoretical proof, however, is still lacking.

Whereas the choice of ℓ determines the number of fixed points to be estimated, the choice of how to compose the columns of Ψ is less important. The general representation of matrix Ψ is

$$\Psi = \begin{bmatrix} 1 & y(k-1) & \cdots & y(k-n_1) & y(k-1)^2 \\ 1 & y(k+1-1) & \cdots & y(k+1-n_1) & y(k+1-1)^2 \\ \vdots & \vdots & \vdots & \vdots & \vdots \\ 1 & y(k+L-1-1) & \cdots & y(k+L-1-n_1) & y(k+L-1-1)^2 \end{bmatrix}$$

$$\begin{bmatrix} \cdots & y(k-n_2)^2 & \cdots & y(k-1)^\ell & \cdots & y(k-n_\ell)^\ell \\ \cdots & y(k+1-n_2)^2 & \cdots & y(k+1-1)^\ell & \cdots & y(k+1-n_\ell)^\ell \\ \vdots & \vdots & \vdots & \vdots & \vdots & \vdots \\ \cdots & y(k+L-1-n_2)^2 & \cdots & y(k+L-1-1)^\ell & \cdots & y(k+L-1-n_\ell)^\ell \end{bmatrix}. \quad (10)$$

It should be noted that in the matrix above, the range $\{y(k-1)^\ell \ \ldots \ y(k-n_\ell)^\ell\}$ denotes all possible combinations of the monomials $\{y(k-1) \ \ldots \ y(k-n_\ell)\}$ grouped in powers of ℓ, that is the term $y(k-1)y(k-2)$ is contained in $\{y(k-1)^2 \ \cdots \ y(k-n_2)^2\}$. As mentioned above, not all such monomials will ever be used, as illustrated in the examples. Also,

$$\mathbf{y}^T = [y(k) \ y(k+1) \ \cdots \ y(k+L-1)]. \quad (11)$$

Remark 5. The algorithm described above is surprisingly robust to noise (see last example). This robustness is a result of the least-squares estimate performed in Step 5, instead of finding an exact solution as in Eq. (8). Although noise might induce some bias in the parameters the fixed points are still adequately estimated. However, should the fixed points become severely biased due to noise-induced parameter bias, an extended least-squares algorithm can be easily implemented [Norton, 1986].

Remark 6. As will be illustrated in the following section, the last step in the algorithm is just a fine-tuning. Even if Step 9 is not performed, acceptable estimates of fixed points are obtained. However, if spurious clusters are detected and deleted, greater accuracy is readily attained.

4. Numerical Examples

This section illustrates how the algorithm presented in Sec. 3.2 can be used to estimate fixed points from data. Three well known systems are considered, viz. Rössler, Lorenz and Chua's circuit. For the latter, real data are used. In all the examples, the sampling time was chosen according to [Aguirre, 1995], but several tests have shown that this choice is not at all critical in general. In all the examples below, the following regressors were used to form matrix Ψ the first time Step 4 of the algorithm was performed: constant, $y(k-1)$, $y(k-2)$, $y(k-3)$, $y(k-4)$, $y(k-1)^2$, $y(k-2)^2$, $y(k-1)y(k-2)$, $y(k-3)y(k-4)$, $y(k-1)^3$, $y(k-1)y(k-2)^2$, $y(k-3)^3$ and $y(k-1)y(k-2)y(k-3)$, thus $n_\theta = 13$. These regressors were selected rather arbitrarily. The only caution was to make sure that in the first iteration, Ψ would include regressors of each cluster. The fact that the same set of regressors was used for very different systems confirms that the choice is not critical. This is exactly the opposite to the problem of

[1] If the problem at hand were that of model building, for $\ell = 3$ and maximum lags also equal to three, the number of possible terms would be 84, which could be combined in a huge number of ways.

global model building in which the choice of regressors is highly critical.

4.1. *The Rössler equations*

This example uses Rössler's equation defined as [Rössler, 1976]

$$\begin{cases} \dot{x} = -(y+z) \\ \dot{y} = x + \alpha y \\ \dot{z} = \alpha + z(x-\mu)\,, \end{cases} \tag{12}$$

with $\alpha = 0.2$ and $\mu = 5.7$. This system has two fixed points at $(\overline{x}, \overline{y}, \overline{z}) = \{(0.01, -0.05, 0.05); (5.69, -28.45, 28.45)\}$. An interesting feature in this system is that one of the fixed points is totally out of the data range. Thus virtually no information of it is conveyed by the data.

The original time series had $N = 5000$ data points of the x variable sampled at $T_s = 0.08$ with window increment equal to $\Delta = 5$. In this case the window length was $L = 900$ samples wide.

Following the steps outlined in Sec. 3.2 it became clear that all clusters but Ω_y were unnecessary. This can be seen from Fig. 1. As suggested in the new algorithm, retaining the second, third, fourth and fifth columns of matrix Ψ, yields an algebraic equation [see (5)] which only has a trivial root. Therefore, in this case, the (almost) trivial fixed point seems to be the only singularity which can be directly estimated from the data. The algorithm of Glover and Mees [1992] also estimates a single, trivial, fixed point.

4.2. *The Lorenz equations*

This example uses the well-known Lorenz equations [Lorenz, 1963]

$$\begin{cases} \dot{x} = \sigma(y-x) \\ \dot{y} = \rho x - y - xz \\ \dot{z} = xy - \beta z\,, \end{cases} \tag{13}$$

with $\sigma = 10$, $\beta = 8/3$ and $\rho = 28$. This system has fixed points at $(\overline{x}, \overline{y}, \overline{z}) = \{(8.49, -8.49, 27); (-8.49, 8.49, 27); (0, 0, 0)\}$. Equation (13) was simulated and time series with $N = 5000$ of the x component sampled at $T_s = 0.04$ was used to estimate the system fixed points. The window increment was $\Delta = 5$. The fixed points are estimated from the family of algebraic equations such as (5) obtained by estimating parameters for each of the

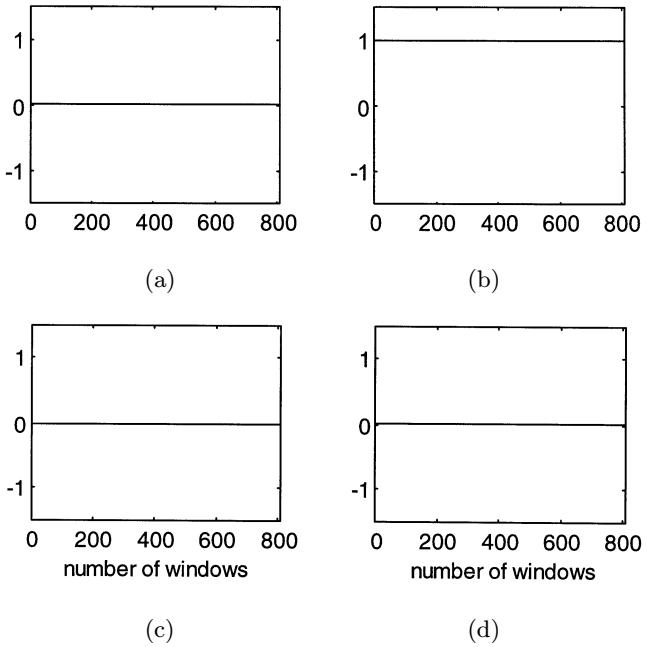

Fig. 1. Estimated cluster coefficients for the Rössler attractor as a result of Step 5. (a) Σ_0, (b) Σ_y, (c) Σ_{y^2}, (d) Σ_{y^3}.

800 windows of data considered with all the columns of Ψ. The estimated fixed points were $\hat{\overline{x}} = \{8.75 \pm 0.13;\ -8.66 \pm 0.11;\ -0.23 \pm 0.27\}$.

From a figure similar to Fig. 1 it became clear that the clusters Ω_0 and Ω_{y^2} were spurious and the respective columns of Ψ were then deleted. As far as fixed points are concerned, this means that the system has a trivial fixed point (as indicated by the statistically insignificant value of the estimated fixed point at -0.23) and is symmetrical. Thus, repeating the same procedure but this time only with some columns of Ψ, the following fixed points were estimated (see also Fig. 2) $\hat{\overline{x}} = \{\pm 8.46 \pm 0.02;\ 0.00\}$. Using the same data, the algorithm by Glover and Mees [1992] did not estimate the trivial fixed point and estimated the following nontrivial singularities: 8.00 ± 0.14 and -8.04 ± 0.18.

An important remark is that this example brought to light two significant properties of the system fixed points, namely (i) the existence of a trivial fixed point and (ii) symmetry with respect to the origin and along the x-axis of the nontrivial fixed points. If this information had been known *a priori* it could have been used from the very start of the fixed point estimation. This shows how the proposed algorithm permits the user to include *a priori* knwoledge.

Another example using this system used a $N = 5000$ data series of the z-component. All

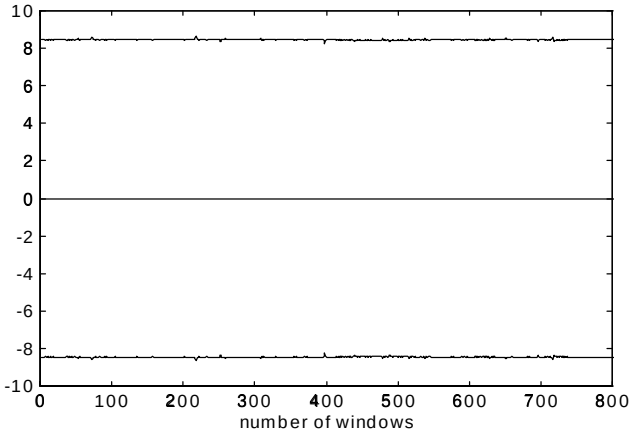

Fig. 2. Estimated fixed points for the Lorenz system estimated from a set of data of the x-coordinate. The data were sectioned in 800 overlapping windows with length $L = 900$.

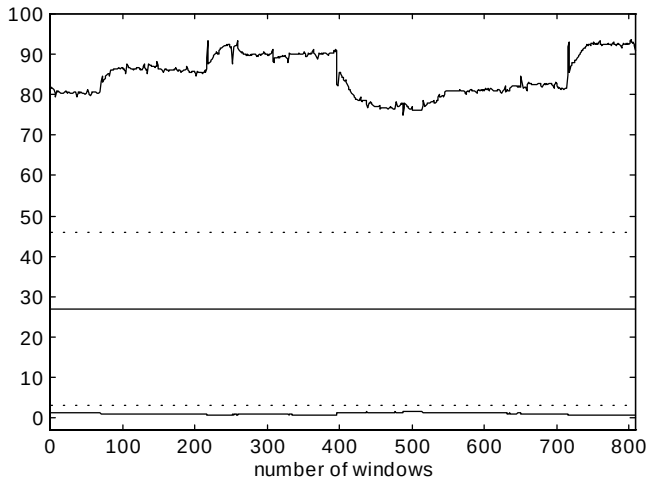

Fig. 3. Fixed points estimated from the z-component of the Lorenz attractor using four columns to compose Ψ. The dashed lines indicate the data limits. One of the fixed points lacks consistence, this being an indication that only two fixed points can be reliably estimated from the data. This suggests that $\ell = 2$ and not $\ell = 3$ (i.e. deletion of the fourth column of Ψ).

other parameter values, e.g. L, Δ, etc. were as before. The fixed points estimated from these data are shown in Fig. 3 together with the data range limits. From this figure, it seems that one fixed point is spurious because of the corresponding large variance plus the fact that the estimated values are well outside the data range limits. Also, from cluster analysis analogous to the one carried out for the Rössler equations, it can be deduced that Ω_0 is also spurious. Thus, removing the columns of Ψ that correspond to Ω_0 and Ω_{y^3}, the following fixed points were

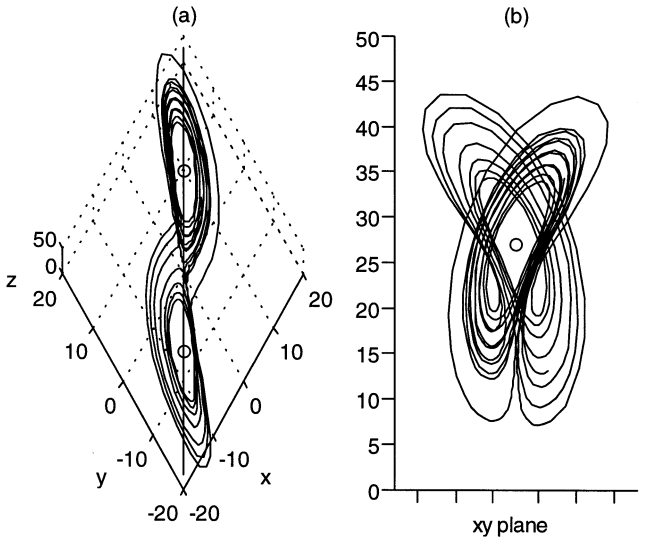

Fig. 4. Lorenz attractor. (b) is a view of (a) along the line crossing both nontrivial fixed points. The projections of both such fixed points onto the z-axis concide.

accurately estimated: $\{27.53 \pm 0.05, 0.00\}$. It is interesting to point out that in this particular example the dynamics have a *rational* form (and not polynomial), therefore suggesting that the dynamics need not be necessarily polynomial for the algorithm to perform well.

An interesting remark is that although the Lorenz system has three fixed points which were successfully estimated from a time series of the x-component, from the observation of the z-component only two fixed points are *seen* by the algorithm. The explanation for this is simple and is illustrated in Fig. 4. As can be seen from this figure, the projections of the nontrivial fixed points onto the z-axis coincide, thus from observations of this coordinate, both nontrivial fixed points seem to be just one.

4.3. *Chua's circuit*

The equations which describe Chua's circuit, probably the most popular benchmark for studying nonlinear oscillations [Chua & Hasler, 1993], are

$$\begin{aligned} C_1 \frac{dv_1}{dt} &= \frac{(v_2 - v_1)}{R} - i_{\rm d}(v_1) \\ C_2 \frac{dv_2}{dt} &= \frac{(v_1 - v_2)}{R} + i_L \\ L \frac{di_L}{dt} &= -v_2 \end{aligned} \tag{14}$$

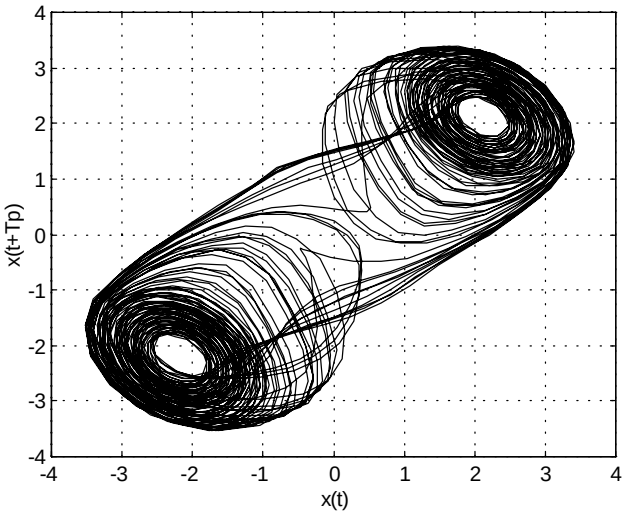

Fig. 5. The double scroll attractor reconstructed from measurements of the voltage across C_1.

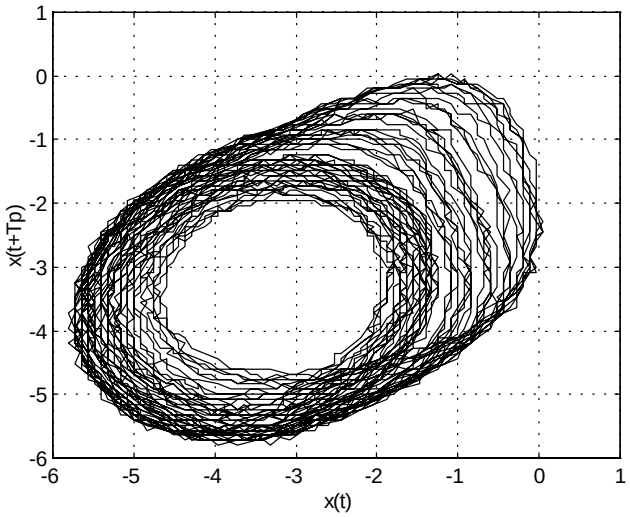

Fig. 6. Chua's spiral attractor. The resolution used was smaller than the one employed to measure the data in Fig. 5.

where v_i is the voltage across capacitor C_i, i_L is the current through the inductor and the current through Chua's diode, the only nonlinear part of the circuit, is given by

$$i_{\rm d}(v_1) = \begin{cases} m_0 v_1 + B_{\rm p}(m_0 - m_1) & v_1 < -B_{\rm p} \\ m_1 v_1 & |v_1| \leq B_{\rm p} \\ m_0 v_1 + B_{\rm p}(m_1 - m_0) & v_1 > -B_{\rm p} \end{cases} \quad (15)$$

where $B_{\rm p}$, m_0 and m_1 are, respectively the break point and the inclinations of the piecewise-linear function of Eq. (15). Time series of the voltage across C_1, measured directly from a real implementation of this circuit, were used to test the new fixed point estimation algorithm.

The first set of data were taken from the double scroll attractor, see Fig. 5. The original time series had $N = 5000$ data points sampled at $T_{\rm s} = 2\mu$s. In this case the window length was $L = 900$ samples wide with $\Delta = 5$. The fixed points estimated at this point were: $\{-2.24 \pm 0.02,\ 0.03 \pm 0.12,\ 2.15 \pm 0.02\}$ V. The algorithm by Glover and Mees [1992] finds slightly unsymmetrical nontrivial fixed points at $\{2.12 \pm 0.06; -2.20 \pm 0.06\}$ V and is rather uncertain about the trivial fixed point. Finally, it is mentioned that dynamically valid models of this attractor have been identified from the same set of data and such models have the following fixed points [Aguirre *et al.*, 1997]: $\{2.21, 0.00, -2.27\}$ V for one model and $\{\pm 2.24, 0.00\}$ V for another model. As can be seen, good agreement was attained.

A figure similar to Fig. 1 clearly revealed that clusters Ω_0 and Ω_{y^2} were spurious, confirming previous results [Aguirre *et al.*, 1997]. Thus eliminating the corresponding columns of Ψ, the following *symmetrical* fixed points were estimated: $\{\pm 2.20 \pm 0.01, 0.00\}$ V.

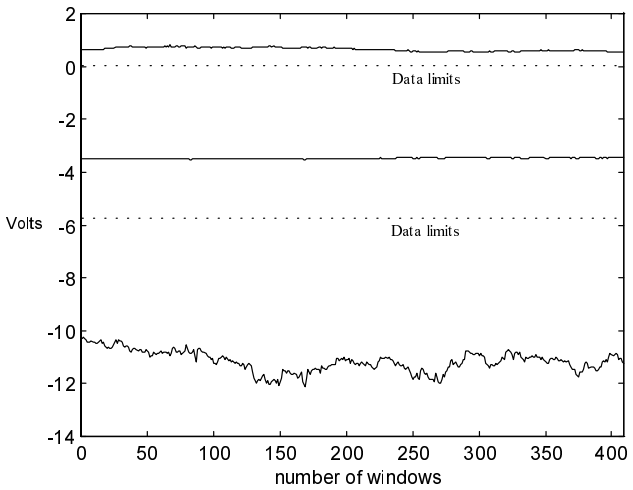

Fig. 7. Fixed points estimated from data on the spiral attractor. This result suggests that only two fixed points can be reliably estimated.

In the sequel, 3000 data points were taken from Chua's spiral attractor (see Fig. 6). The sampling time and the window length were $T_{\rm s} = 20\mu$s and $L = 900$, respectively with $\Delta = 5$.

Figure 7 shows the fixed points estimated by the new algorithm using all the columns of Ψ. As can be noticed, the variance of one fixed point is much greater than the others plus the estimated value is outside the data limits (which oscillate roughly between -6 and 0). Based on this information, it can be safely concluded that the

algorithm can only estimate two fixed points and therefore the 10th to 13th columns of Ψ (which corresponds to Ω_{y^3}) should be removed. Doing this the following fixed points were finally estimated: $\{-3.65 \pm 0.02,\ 0.00\}$ V. Glover and Mees' algorithm failed to indicate any fixed points from the set of data used.

Finally, we investigate the influence of noise. It should be noticed that the data shown in Figs. 5 and 6 were obtained from real measurements thus they do contain a realistic amount of noise. However, extra noise was added with increasing variance and fixed points estimated in order to assess the algorithm robustness with respect to additive noise. The results are summarized in Fig. 8. Figure 9 shows the measured double scroll corrupted with extra additive noise of variance $\sigma_e^2 = 0.3$. This example shows that even for badly corrupted data, the new algorithm estimates fixed points with good accuracy.

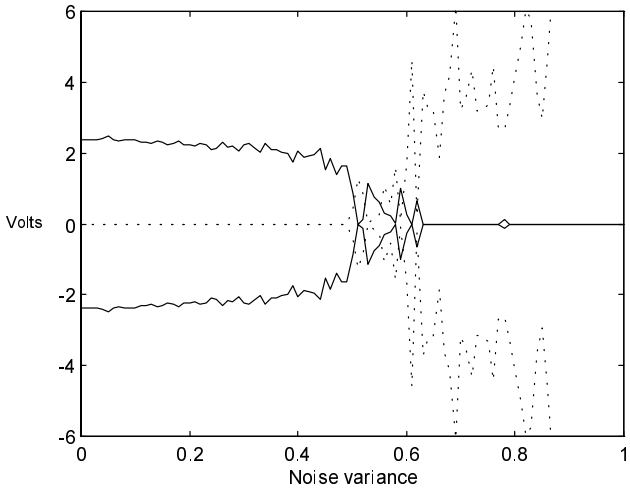

Fig. 8. Nontrivial fixed points estimated from the double scroll data corrupted with increasing noise variance. Reasonably good estimates were obtained for noise variances up to 0.4. The dashed lines indicate the imaginary parts of the fixed points whilst the solid lines indicate the real parts.

4.4. *Limit-cycle estimation an example from the Rössler system*

The fixed-point estimation algorithm described in Sec. 3.2 can be used to estimate limit cycles from data in a two-step procedure as follows. First, the data should be Poincaré-sampled in such a way that the resulting data correspond to the n_{p}th return map with $n_{\mathrm{p}} = 1, 2, \ldots$. Second, run the algorithm of Sec. 3.2 on the sampled data. Clearly, a fixed point on the n_{p}th return map will correspond to an n_{p}-period limit circle.

Although quite effective, the procedure above suffers from the curse of dimensionality. In other words, in order to be able to estimate n_{p}-period limit circles a fair amount of data is usually required. Specifically, it is helpful to have at least 1000 data points to work with. Thus, if the sampling time is chosen in such a way as to have around 100 samples per pseudo-period, and recalling that n_{p} pseudo-periods are required to have one Poincaré sample on the n_{p}th return map, then the original time series should have about $1000 \times 100 \times n_{\mathrm{p}} = n_{\mathrm{p}} \times 10^5$ data points. On the other hand, an advantage of this new procedure, especially over other "box-counting" algorithms, is that strongly unstable limit cycles can be estimated with greater ease. This is a consequence of estimating fixed points using the model structure rather than monitoring the trajectory of the system in the embedding space. In the latter case, if a limit cycle is strongly

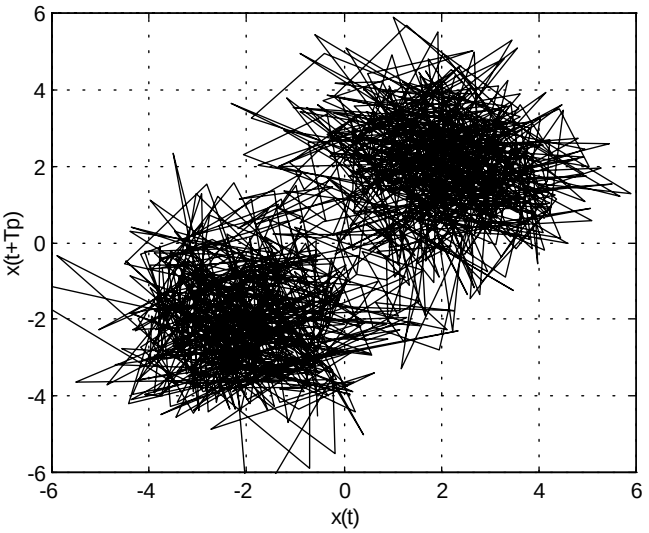

Fig. 9. Double scroll attractor corrupted with noise with variance equal to 0.3.

unstable, it is very unlikely that the system will stay close to such a limit cycle long enough to enable the algorithm to detect the limit cycle.

In this example the Rössler system was used to generate data. Box-counting algorithms [Lathorp & Kostelich, 1989] were used to find pseudo-periodic orbits as shown in Fig. 10(a). This figure clearly indicates the presence of period-two and period-three orbits (limit cycles with higher periodicity do exist but are not shown in the figure). The box-counting algorithm used with $\varepsilon = 0.02$ did not detect the period-one limit cycle, perhaps due to strong

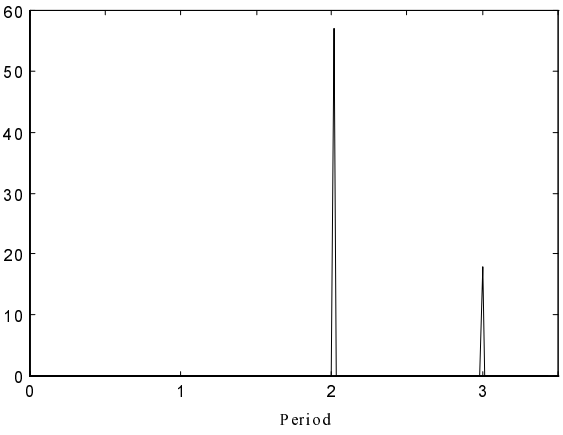

(a)

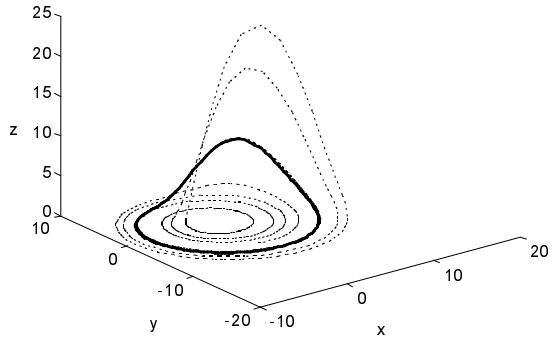

(b)

Fig. 10. Pseudo-periodic orbits in the Rössler attractor. (a) The box-counting algorithm used did not find any limit cycle of period-one. (b) The heavy line was obtained simulating the Rössler system starting close to a period-one limit cycle found using the algorithm described in Sec. 3.2. This suggests that there is a period-one unstable limit cycle close to the orbit indicated with heavy line.

instability. Another reason for this is that because of the initial conditions the time series used might have had very little information about such a limit cycle.

The original time-series was then Poincaré-sampled at $x = 0$ and the resulting first-return map data was used to feed the algorithm described in Sec. 3.2. Such an algorithm found the following fixed point: $\{y, z\} = \{-8.4065 \pm 0.0064, 0.02971 \pm 0.00003\}$. Thus using the point $\{x, y, z\} = \{0, -8.4065, 0.02971\}$ as initial condition, the orbit shown in Fig. 10(b) was obtained via simulation. Clearly, this is a pseudo-periodic orbit located very close to an unstable limit cycle with periodicity one. Of course, after some few iterations this orbit wanders away from the unstable limit cycle.

The objective of this example was to illustrate a potential use of the new algorithm. There are, of course, more simple ways to estimate the fixed points of Poincaré maps of the Rössler system [Letellier *et al.*, 1995].

5. Conclusions

A new fixed point estimation algorithm has been presented.[2] This algorithm is extremely simple and works by first estimating a limited number of parameters and subsequently calculating the fixed points from such parameters. The algorithm has some attractive features: (i) absolutely no structure selection is required, thus avoiding one of the most difficult problems in nonlinear model building, (ii) more than one fixed point can be estimated at a time, and (iii) *a priori* information can sometimes be incorporated to enhance fixed point estimation. *The price paid for such a simple algorithm is that the estimated nonlinear structure is not a model of the underlying dynamics.* A by-product of the novel procedure is a cluster analysis of the data. Such analysis may give the user some hints concerning the number, symmetry and possible existence of a trivial fixed point. The new algorithm has been tested in a number of well-known benchmark systems using both simulated and real data.

Acknowledgments

Financial support from CNPq, FAPEMIG and PRPq/UFMG is gratefully acknowledged. The authors are grateful to Leonardo Torres and Giovani Rodrigues for valuable help.

References

Aguirre, L. A. [1995] "A nonlinear correlation function for selecting the delay time in dynamical reconstructions," *Phys. Lett.* **A203**(2,3), 88–94.

Aguirre, L. A. & Billings, S. A. [1995] "Improved structure selection for nonlinear models based on term clustering," *Int. J. Control* **62**(3), 569–587.

Aguirre, L. A. & Mendes, E. M. [1996] "Nonlinear polynomial models: Structure, term clusters and fixed points," *Int. J. Bifurcation and Chaos* **6**(2), 279–294.

[2]A copy of the Matlab code can be downloaded from http://www.cpdee.ufmg.br/~MACSIN.

Aguirre, L. A., Rodrigues, G. G. & Mendes, E. M. [1997] "Nonlinear identification and cluster analysis of chaotic attractors from a real implementation of Chua's circuit," *Int. J. Bifurcation and Chaos* **7**(6), 1411–1423.

Chen, G. [1999] "Chaos, bifurcations and their control," in *Wiley Encyclopedia of Electrical and Electronics Engineering* (John Wiley).

Chua, L. O. & Hasler, M. (Guest Eds.) [1993] Special issue on chaos in nonlinear electronic circuits, *IEEE Trans. Circuits Syst.* **40**(10,11).

Fujisaka, H. & Sato, C. [1997] "Computing the number, location and stability of fixed points of Poincaré maps," *IEEE Trans. Circuits Syst. I* **44**(4), 303–311.

Glover, J. & Mees, A. [1992] "Reconstructing the dynamics of Chua's circuit," *J. Circuits Syst. Comput.* **3**, 201–214.

Kugiumtzis, D. [1996] "State space reconstruction parameters in the analysis of chaotic time series — the role of time series length," *Physica* **D95**, 13–28.

Lathorp, D. P. & Kostelich, E. J. [1989] "Characterization of an experimental strange attractor by periodic orbits," *Phys. Rev.* **A40**(7), 4028–4031.

Letellier, C., Dutertre, P. & Maheu, B. [1995] "Unstable periodic orbits and templates of the Rössler system: Toward a systematic topological characterization," *Chaos* **5**(1), 271–282.

Lorenz, E. [1963] "Deterministic nonperiodic flow," *J. Atmos. Sci.* **20**, 282–293.

Norton, J. P. [1986] *An Introduction to Identification* (Academic Press, London).

Rössler, O. E. [1976] "An equation for continuous chaos," *Phys. Lett.* **A57**(5), 397–398.